

# Gold-Nanocluster-Doped Inorganic–Organic Hybrid Coatings on Polycarbonate and Isolation of Shaped Gold Microcrystals from the Coating Sol

Goutam De\* and Debtosh Kundu

Sol-Gel Division, Central Glass and Ceramic Research Institute, 196, Raja S.C. Mullick Road, Jadavpur, Kolkata 700 032, India

Received January 23, 2001. Revised Manuscript Received July 2, 2001

Au-nanocluster-doped inorganic–organic hybrid coatings on polycarbonate substrates were prepared for the application of abrasion-resistant colored coatings as well as nonlinear optical material. The Au-doped sol was prepared by incorporating  $\text{HAuCl}_4 \cdot 4\text{H}_2\text{O}$  into a composite sol derived from 3-(glycidoxypropyl)trimethoxysilane, tetraethylorthosilicate, and 3-(methacryloxypropyl)trimethoxysilane via hydrolysis–condensation and epoxy polymerization reactions. When the coated substrates were exposed under UV light, three reactions occurred simultaneously: (i) reduction of Au ions into metallic Au nanoclusters, (ii) polymerization of methacrylate groups, and (iii) strengthening of the silica network. As a result, the UV-cured coatings became reddish-purple and more abrasion-resistant than the polycarbonate substrate. UV–vis spectroscopy and TEM of the films showed a peak at 530 nm due to the surface plasmon resonance of Au nanoclusters and the presence of 8–10 nm spherical Au nanoclusters, respectively. XRD of the films also showed the characteristic peaks of metallic Au nanoclusters. The inorganic–organic hybrid network at the sol stage also acted as a new breeding medium for the generation of shaped (triangular, hexagonal, prismatic, etc.) Au microcrystals from the Au-doped sol without UV irradiation. Electron diffraction suggests that these were single crystals with a preferential growth along the Au (111) plane.

## Introduction

At the molecular level, inorganic–organic hybrid coatings show promising applications as hard and abrasion-resistant coatings on plastic substrates.<sup>1–6</sup> In addition, hybrid materials are considered to be the next-generation composite materials having a wide variety of applications<sup>7–16</sup> as, for example, mesoporous materi-

als through surfactant templates,<sup>10,11</sup> heterogeneous biocatalysts,<sup>12</sup> optical waveguides,<sup>13</sup> contact lens materials,<sup>14</sup> and bioactive materials.<sup>15</sup>

3-(Glycidoxypropyl)trimethoxysilane (GLYMO) and 3-(methacryloxypropyl)trimethoxysilane (MEMO) have been largely used as precursors for inorganic–organic hybrid sol–gel materials.<sup>1,2,9,17</sup> Both GLYMO and MEMO have the ability to form simultaneously an inorganic network,  $\equiv\text{Si}-\text{O}-\text{Si}\equiv$ , through hydrolysis and condensation reactions of the alkoxy groups and organic network, poly(ethylene oxide) and polymethacrylate, through the polymerization of epoxy and methacrylate groups, respectively.

In this paper we report Au-nanocluster-incorporated, hard inorganic–organic coatings on transparent polycarbonate (PC) substrates.<sup>18</sup> Here, “dual organic functionality” i.e., the epoxy units of GLYMO (heat sensitive) and the methacrylate units of MEMO (light sensitive), is utilized for the organic part of the coatings. The inorganic part constitutes with the “silica” from GLYMO

\* Corresponding author. Fax: +91 33 4730957. E-mail: gde41@hotmail.com.

(1) Nass, R.; Arpac, E.; Glaubitt, W.; Schmidt, H. *J. Non-Cryst. Solids* **1990**, *121*, 370. (b) Schmidt, H. *J. Non-Cryst. Solids*, **1994**, *178*, 302. (c) Wen, J.; Jordens, K.; Wilkes, G. L. *Mater. Res. Soc. Symp. Proc.* **1996**, *435*, 207. (d) Schmidt, H. K.; Geiter, E.; Mennig, M.; Krug, H.; Becker C.; Winkler, R.-P. *J. Sol-Gel Sci. Technol.* **1998**, *13*, 397. (e) Sempere, S.; Kunze, N.; Werner, B.; Schmidt, H. In *Coatings on Glass*; Pulker, H., Schmidt, H., Aegerter, M. A., Eds.; Proc. 2nd Int. Conf. On Coatings on Glass (Saarbruecken, Germany); 1998; pp 319–322.

(2) Floch, H. G.; Belleville, P. F. *J. Sol-Gel Sci. Technol.* **1994**, *1*, 293.

(3) (a) Etienne, P.; Sempere, R.; Phalippou, J. *J. Sol-Gel Sci. Technol.* **1994**, *2*, 171. (b) Etienne, P.; Denape, J.; Paris, J. Y.; Phalippou, J.; Sempere, R. *J. Sol-Gel Sci. Technol.* **1996**, *6*, 287.

(4) (a) Betrabet, C.; Wikes, G. L. *Am. Chem. Soc. Polym. Prepr.* **1992**, *33*, 286. (b) Wang, B.; Wikes, G. L. *J. Macromol. Sci. Pure Appl. Chem.* **1994**, *A31*, 249.

(5) Wold, C. R.; Soucek, M. D. *J. Coat. Technol.* **1998**, *70*, 43.

(6) Del Monte, F.; Cheben, P.; Grover, C. P.; Mackenzie, J. D. *J. Sol-Gel Sci. Technol.* **1999**, *15*, 73.

(7) Novak, B. M. *Adv. Mater.* **1993**, *5*, 422.

(8) Judeinstein, P.; Sanchez, C. *J. Mater. Chem.* **1996**, *6*, 511.

(9) Chujo, Y. *Curr. Opin. Solid State Mater. Sci.* **1996**, *1*, 806.

(10) Sims, S. D.; Berkett, S. L.; Mann, S. *Mater. Res. Soc. Symp. Proc.* **1996**, *431*, 77.

(11) Burkett, S. L.; Sims, S. D.; Mann, S. *Chem. Commun.* **1996**, 1367.

(12) Reetz, M. T.; Zonta, A.; Simpelkamp, J. *Angew. Chem. Int. Ed.* **1995**, *34*, 301.

(13) Zevin, M.; Reisfeld, R. *Opt. Mater.* **1997**, *8*, 37.

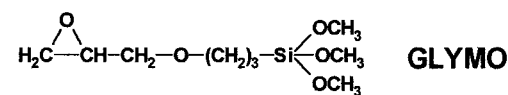
(14) Philipp, G.; Schmidt, H. *J. Non-Cryst. Solids* **1984**, *63*, 283.

(15) Yabuta, T.; Tsuru, K.; Hayakawa, S.; Ohtsuki, C.; Osaka, A. *J. Sol-Gel Sci. and Technol.* **2000**, *19*, 745.

(16) Sanchez, C.; Lebeau, B.; Ribot, F.; In, M. *J. Sol-Gel Sci. Technol.* **2000**, *19*, 745.

(17) Innocenzi, P.; Brusatin, G.; Guglielmi, M.; Bertani, R. *Chem. Mater.* **1999**, *11*, 1672.

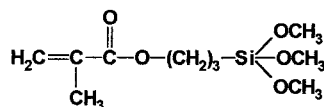
(18) The polycarbonate substrates have several unique properties, e.g., excellent clarity, complete UV cutoff, self-extinguishing, heat resistant up to 120 °C, can withstand 250 times greater impact than glass (i.e. virtually unbreakable), but they are not scratch resistant enough for practical applications such as transparent windows and optical lens.



'Epoxy'  
Polymerizable  
Organic Part

Hydrolyzable  
'Alkoxy'  
Groups

GLYMO



'Methacrylate'  
Polymerizable  
Organic Part

Hydrolyzable  
'Alkoxy'  
Groups

MEMO

and MEMO, as well as tetraethylorthosilicate (TEOS). Finally, Au nanoclusters are generated in the hybrid matrix, which make the coatings reddish purple in color, due to the surface plasmon resonance (SPR) of Au nanoclusters.<sup>19</sup> These colored inorganic–organic hybrid abrasion-resistant coatings on PC are applicable to both indoor and outdoor decorative purposes.

It is also known that the presence of nanoclusters in a dielectric matrix enhances the third-order electronic susceptibility,  $\chi^{(3)}$ , of the host by several orders of magnitude.<sup>19,20</sup> Such materials are particularly promising for optoelectronics, aiming to design all-optical switching devices. However, research on the Au-nanocluster-doped sol–gel coatings is mostly confined to glassy matrixes and glass substrates.<sup>19,20</sup> Therefore, the Au-nanocluster-doped inorganic–organic hybrid coatings on PC developed in this work may also be useful as an alternative nonlinear optical material.

It is widely known that shape-controlled Au microcrystals can be obtained from an aqueous solution of  $\text{HAuCl}_4$ <sup>21–24</sup> either by reduction with a suitable reducing agent, e.g., sodium citrate,<sup>21</sup> citric acid,<sup>21</sup> sodium borohydride,<sup>22</sup> and pyrrole,<sup>22</sup> or UV light.<sup>23,24</sup> The sodium borohydride and pyrrole reductions were employed for the synthesis of thiol-stabilized Au nanoparticles.<sup>22</sup> It has also been found that the rodlike micelles of hexadecyltrimethylammonium chloride operates as a template for the preparation of spherical to needle-shaped gold crystals from  $\text{HAuCl}_4$  solution following a UV irradiation technique.<sup>23</sup> In the present study, we found that gold microcrystals of different shapes were separated out from the coating sol during storage. Accord-

ingly, we also report here for the first time the formation of Au microcrystals from Au-doped inorganic–organic hybrid sols.

## Experimental Section

**Preparation of Sols.** GLYMO (60 mmol) and TEOS (35 mmol) were first cohydrolyzed in the presence of hydrochloric acid (0.185 mmol) and water (150 mmol). The above liquid mixture was stirred at room temperature ( $26 \pm 1$  °C) for 1 h. During this period, the initial heterogeneous liquid mixture transformed to a homogeneous sol. The sol was then refluxed for 2 h at 80.5 °C.<sup>25</sup> This refluxed sol was then cooled to  $26 \pm 1$  °C, and a 1:1 (by volume) methanol solution of MEMO (20 mmol) and water (50 mmol) mixture was added under stirring. Stirring was continued for 1 h and the solution was refluxed again for 1 h at 72.5 °C<sup>25</sup> to obtain a composite GLYMO–TEOS–MEMO sol. The molar ratio of GLYMO:TEOS:MEMO was 3:1.75:1. To this composite 1-methylimidazole (8 mmol; dissolved in 150 mmol methanol) was added as an epoxy polymerization initiators. The sol was then refluxed for 1 h at 68 °C<sup>25</sup> to polymerize the epoxy groups. A faint yellowish sol resulted. Finally, methacrylate polymerization initiator, benzyl (0.027 mmol), was added, and the sol was aged at room temperature for 48 h. This sol is designated as GTM sol.

The Au-doped coating sol (Au-GTM sol) was prepared by incorporating  $\text{HAuCl}_4 \cdot 4\text{H}_2\text{O}$  (4.0 mmol; dissolved in 90–125 mmol of methanol) into the GTM sol under stirring. The stirring was continued for 2 h, and the resulting yellow sol was left undisturbed and sealed for 16 h prior to use as a coating sol. The composition with respect to the equivalent gold metal and silica in the sol was 3.4 mol % Au, 96.6 mol %  $\text{SiO}_2$ .

**Preparation of Coatings.** The coatings were prepared from the GTM and Au-GTM sols on 3 mm thick transparent PC substrates (Lexan, GE plastics).<sup>26</sup> Prior to the coating deposition, the PC substrates were first cleaned with a neutral detergent, followed by rinsing with distilled water and 2-propanol, and finally, boiled in 2-propanol for 5 min. The coatings were prepared using the dipping technique (Dip-master 200, Chemat Corporation) with withdrawal velocities in the range of 2–20 cm/min. Similar coatings on pure silica glass and silicon wafers (both sides polished) were also prepared for the UV–visible and IR spectral studies, respectively.

**Curing of the Coatings.** The coatings were first dried at 60 °C in an air oven and then cured 5–20 s photochemically using UV light (Hg vapor lamp through silica glass tube), followed by thermal curing at 100 °C for 1 h. The UV curing was done by passing the oven-dried coated samples through the silica tube (UV light enters the silica tube from the Hg vapor lamp) with a velocity of 2 cm/s, covering a distance of 10 cm. The UV light is focused in such a way that it covers only the 10 cm central part of the silica tube. In this way a UV exposure of 5 s can be obtained by a single operation. This step was repeated up to four times to increase the UV exposure time.

**Gold Microcrystals from the Coating Sols.** When the Au-GTM coating sol was stored under closed conditions (at 25 °C in absence of the light) for about 3–5 days,<sup>27</sup> precipitation of gold microcrystals was observed. The intensity of the yellow

(19) Gonella, F.; Mazzoldi, P. Metal Nanocluster Composite Glasses. In *Handbook of Nanostructured Materials and Nanotechnology*; Nalwa, H. S., Ed.; Academic Press: San Diego, 2000; Vol. 4, pp 81–158.

(20) (a) De, G.; Mattei, G.; Mazzoldi, P.; Sada, C.; Battaglin, G.; Quaranta, A. *Chem. Mater.* **2000**, *12*, 2157. (b) Fukumi, K.; Chayahara, A.; Kadono, K.; Sakaguchi, T.; Hirono, Y.; Miya, M.; Hayakawa, J.; Satou, M. *Jpn. J. Appl. Phys.* **1991**, *30*, L742. (c) Matsuoka, J.; Mizutani, R.; Kaneko, S.; Nasu, H.; Kamiya, K.; Kadono, K.; Sakaguchi, T.; Miya, M. *J. Jpn. Ceram. Soc.* **1993**, *101*, 105. (d) De, G.; Tapfer, L.; Catalano, M.; Battaglin, G.; Cacavale, F.; Gonella, F.; Mazzoldi, P.; Haglund, R. F., Jr. *Appl. Phys. Lett.* **1996**, *68*, 3820. (e) Kundu, D.; Honma, I.; Osawa, T.; Komiyama, H. *J. Am. Ceram. Soc.* **1994**, *77*, 1110.

(21) (a) Turkevich, J.; Stevenson, P. C.; Hiller, J. *J. Discuss. Faraday Soc.* **1951**, *11*, 55. (b) Milligan, W. O.; Morriss, R. H. *J. Am. Chem. Soc.* **1964**, *86*, 3461.

(22) (a) Selvan, S. T. *Chem. Commun.* **1998**, 351. (b) Torigoe, K.; Esumi, K. *J. Phys. Chem. B* **1999**, *203*, 2862.

(23) Esumi, K.; Matshuhisa, K.; Torigoe, K. *Langmuir* **1995**, *11*, 3285.

(24) Y. Zhou, C. Y. Wang, Y. R. Zhu, and Z. Y. Chen, *Chem. Mater.* **1998**, *11*, 2310.

(25) All the precursors used here have boiling points much higher than 80.5 °C. However, the boiling temperature of this liquid mixture becomes 80.5 °C due to the generation of methanol and ethanol during the course of hydrolysis and condensation reactions of alkoxy ( $-\text{OCH}_3$  and  $-\text{OC}_2\text{H}_5$ ) groups following the equation  $\equiv\text{Si}-\text{OCH}_3/\text{OC}_2\text{H}_5 + \text{H}_2\text{O} \rightarrow \equiv\text{Si}-\text{OH} + \text{CH}_3\text{OH}/\text{C}_2\text{H}_5\text{OH}$ . Further lowering of refluxing temperatures to 72.5 °C and 68 °C are due to the addition of extra methanol in the reaction mixture.

(26) Polycarbonates are manufactured by the reaction of bisphenol A and phosgene or diphenyl carbonate. The average molecular weight of this material is between 22 000 and 32 000. For further details, see: Milby, R. V. *Plastics Technology*; McGraw-Hill: New York, 1973; pp 292–294.

(27) We have used 90–125 mmol of methanol to dissolve 4 mmol of  $\text{HAuCl}_4 \cdot 4\text{H}_2\text{O}$ . Use of less methanol (<90 mmol) gives precipitation of gold microcrystals within 3 days.

color of the sol decreased gradually due to the precipitation of Au microcrystals, and colorless sol resulted after about 10 days.

**Surface Profile and Thickness Measurements.** The surface profile and thickness of the cured coatings deposited on polycarbonate and silica substrates were measured by a Surfcoorder SE-2300 profilometer (Kosaka Laboratory Ltd.).

**Infrared Spectroscopy.** Infrared absorption spectra of the sol and films deposited on silicon wafers were recorded by Fourier transform infrared (FTIR) spectrometry (model 5PC, Nicolet) with a resolution of  $4\text{ cm}^{-1}$  and 200 scans for each sample. The sol spectrum was taken by placing the sol between two KBr windows separated by an annular Teflon ring spacer of thickness 0.05 mm.

**UV-Visible Spectroscopy.** The UV-visible absorption spectra (190–800 nm) of the sol and coatings deposited on silica glass and PC substrates were obtained using Shimadzu UV3101PC and Cary50 scan spectrophotometers.

**Transmission Electron Microscopy.** TEM and electron diffraction data were obtained using a JEOL 200CX transmission electron microscope operating at 120 kV. TEM samples were prepared by scraping the cured Au-GTM films deposited on silica glass substrate. The scraped samples were first dispersed in methanol under ultrasonication, and one small drop of this dispersion was deposited onto a carbon-coated grid on an underlying tissue paper. In the case of Au microcrystals, methanol dispersion was directly deposited on a carbon-coated grid in a similar way.

**X-ray Diffraction.** The XRD pattern of the Au-GTM film samples was recorded in a Seifert XRD-3000P diffractometer operating at 30 kV and 30 mA using Ni-filtered Cu  $K\alpha$  radiation. The diffracted X-rays were collected by scanning between  $2\theta = 33^\circ$  and  $2\theta = 55^\circ$  with a step size of  $0.02^\circ 2\theta$  and a dwell time of 5 s per step.

**Scanning Electron Microscopy.** SEM data of the Au microcrystals were obtained using a Leo S430I scanning electron microscope. SEM samples were prepared by spreading the Au microcrystals on a carbon-coated grid.

**Adhesion Test.** An adhesive-tape test was performed following the DIN 53151 specification. The coated surface (20 mm  $\times$  10 mm) was first scratched both horizontally and vertically (2 mm apart) with a steel knife down to the substrate. Second, the scratched surface was covered with Scotch Magic tape (Birla 3M Limited). The tape was then pulled off slowly from the coating at about  $180^\circ$  to the surface.

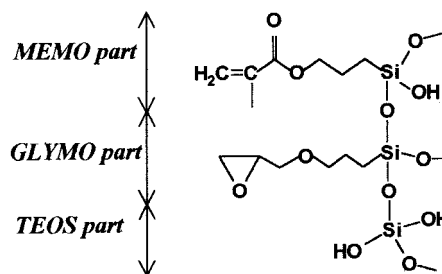
**Abrasion Test.** Abrasion testing of the Au-doped hybrid coatings was performed using a US military specification lens coating hardness tester kit (Summers Optical) in accordance with MIL-F-48616.<sup>2</sup> The kit contains one brass instrument with a spring that was calibrated for 2.5 lbs of pressure.<sup>28</sup> The eraser (rubber–pumice composite) inserts provided with the instrument are manufactured and certified to conform to US federal specification MIL-E-12397B.<sup>28</sup> The test consists of rubbing across the coated surface with the eraser bearing 2.5 lbs of pressure. 2-Propanol was used to clean the coated surface before and after tests. Similar tests were also performed on the uncoated substrate (PC) and undoped coatings.

## Results and Discussion

GLYMO, TEOS, and MEMO were cohydrolyzed in order to connect them together through a –Si–O–Si– network. Scheme 1 shows a model composite structure formed after hydrolysis and condensation reactions of the alkoxy groups of the precursors. In this scheme, one molecule of each of the precursors is shown. The actual molar stoichiometry of GLYMO:TEOS:MEMO was 3:1.75:1 (see the Experimental Section).

(28) The calibration of the springs in the instrument is traceable to the National Institute of Standards and Technology. The eraser used in this instrument is made of high-grade rubber combined with 50  $\pm$  5% by weight of the abrasives (fine-ground pumice) as filler.

### Scheme 1



### Scheme 2

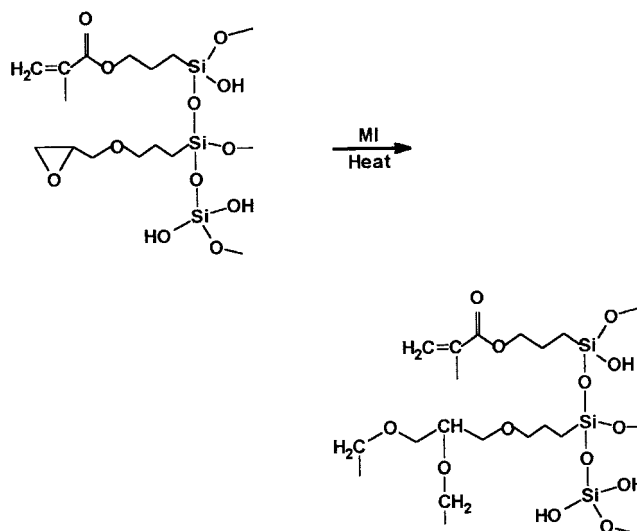


**Table 1. Thickness of the Cured Coatings Obtained from GTM and Au-GTM Sols at Different Withdrawal Velocities**

| withdrawal velocity (cm/min) | coating thickness <sup>a</sup> ( $\mu\text{m}$ ) $\pm$ 0.05 $\mu\text{m}$ |        | withdrawal velocity (cm/min) | coating thickness <sup>a</sup> ( $\mu\text{m}$ ) $\pm$ 0.05 $\mu\text{m}$ |        |
|------------------------------|---|--------|------------------------------|---|--------|
|                              | GTM   | Au-GTM |                              | GTM   | Au-GTM |
| 2                            | 1.70  | 1.40   | 14                           | 6.85  | 4.70   |
| 4                            | 2.50  | 1.90   | 16                           | 7.50  | 5.50   |
| 6                            | 3.30  | 2.55   | 20                           | 8.60  | 6.15   |
| 10                           | 5.10  | 3.60   |                              |   |        |

<sup>a</sup> Average value of three sets of coatings prepared in each withdrawal velocity.

The epoxy groups of GLYMO were then polymerized under reflux using 1-methylimidazole (MI) as the initiator.<sup>17,29</sup> Therefore, at the sol stage, the organic portion of GLYMO polymerizes, as shown in Scheme 2. The methacrylate groups remain in monomeric form, which are then polymerized during UV-curing of the coatings. The coatings prepared from the GTM and Au-GTM sols after UV (20 s), followed by thermal curing (100  $^\circ\text{C}$ ), appeared homogeneous and crack-free and showed excellent clarity with smooth surface. The Au-nanocluster-doped hybrid (Au-GTM) coatings were transparent and reddish-purple in color, whereas the corresponding undoped (GTM) coatings were colorless. The thickness of the coatings can be varied by changing the withdrawal velocities of the substrate from the sol. Table 1 shows some typical thickness data of the GTM and Au-GTM coatings after UV (20 s) and thermal (100  $^\circ\text{C}$ /1 h) curing with respect to the withdrawal velocities of the

(29) Popall, M.; Durand, H. *Electrochim. Acta* **1992**, *37*, 1593.



substrate. The thinner coatings ( $<1 \mu\text{m}$ ) could also be prepared by diluting the sol with methanol. It is important to note that the coating thickness of  $\geq 5 \mu\text{m}$  is appropriate for better abrasion resistance property.

It has been observed that the undoped GTM sol is found to be suitable for coating preparation for more than 3 months if stored under dark and sealed conditions. On the contrary, the Au-GTM sol is suitable for coating preparation for about 2 days, and precipitation of gold microcrystals from the sol was observed visually after about 3–5 days.<sup>27</sup>

**UV-Visible Spectra.** UV-visible absorption spectrum of the Au-GTM sol<sup>30</sup> shows the presence of bands at 225 nm (shoulder) and 320 nm due to the charge transfer between the Au and chloro ligands of  $\text{AuCl}_4^-$  ions.<sup>22b,31</sup> Another band at 207 nm, due to the absorption of C=O groups arising from the  $\alpha,\beta$ -unsaturated groups of MEMO,<sup>33</sup> is also observed. The undoped GTM sol spectrum<sup>30</sup> shows only the presence of the 207 nm band due to C=O absorption. The UV-visible spectra of Au-GTM films deposited on silica glass and polycarbonate substrates are presented in Figures 1–3. Au-GTM coatings deposited (dried at 60 °C for 30 min) on silica glass substrates show strong absorption bands at 225 and 320 nm (Figure 1A, curve a) due to the  $\text{AuCl}_4^-$  ions.<sup>22b,31</sup> In this case the C=O absorption band appeared at 210 nm. The corresponding undoped coating shows only absorption bands correspond to the C=O groups at 210 nm (Figure 2, curve a). Therefore the UV-visible spectral data clearly suggests that (i)  $\text{AuCl}_4^-$  ions are present in the Au-GTM sol and prepared coatings and (ii) the methacrylate unsaturations are present in both the doped and undoped sols and coatings.

When the doped coatings are dried more than 1 h at 60 °C, the bands at 225 and 320 nm disappear (Figure 1A, curve b) indicating the decomposition of the  $\text{AuCl}_4^-$  ions in the coating. However, the 210 nm peak corresponding to the C=O group of the  $\alpha,\beta$ -unsaturated methacrylate ester<sup>31</sup> is still present. The coatings were exposed under UV radiation for 5–20 s after drying at 60 °C for 30 min. It is interesting to note that the UV-treated coatings (deposited on silica glass) show a new set of bands at 225, 235, and 248 nm and a shoulder at about 290 nm, along with a prominent absorption near 530 nm (Figure 1B). The 530 nm band is due to the SPR of Au nanoclusters (Au-SPR).<sup>19,20a–c</sup> The bands at 225, 235, and 248 nm, as well as the C=O band, gradually weakened and finally disappeared during the UV treatment from 5 to 20 s. However, the shoulder peak at about 290 nm and the Au-SPR peak at 530 nm gradually intensified during UV treatment. The corresponding undoped coatings were also UV treated for comparison. In this case, the band due to C=O at 210 nm gradually disappeared (Figure 2) and a new band appeared at about 290 nm. The 290 nm band can be attributed to

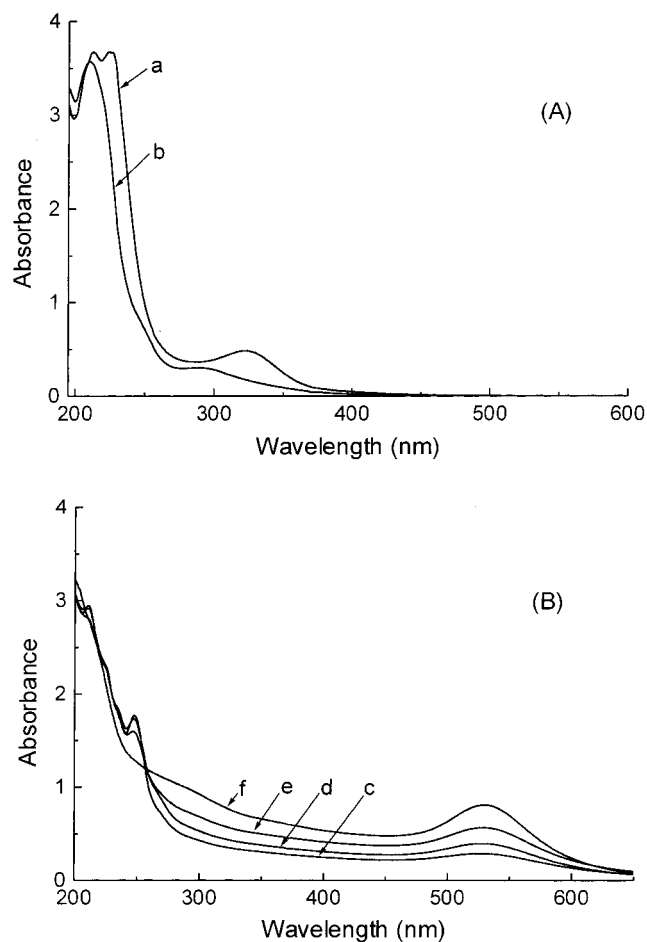


**Figure 1.** UV-visible absorption spectra of Au-GTM films deposited on silica glass with respect to drying and UV curing time: (A) drying at 60 °C for 30 min (a) and 60 min (b); (B) UV curing for 5 s (c), 10 s (d), 15 s (e), and 20 s (f). Film thickness was  $5.0 \mu\text{m}$ , and one side of the substrate was coated.

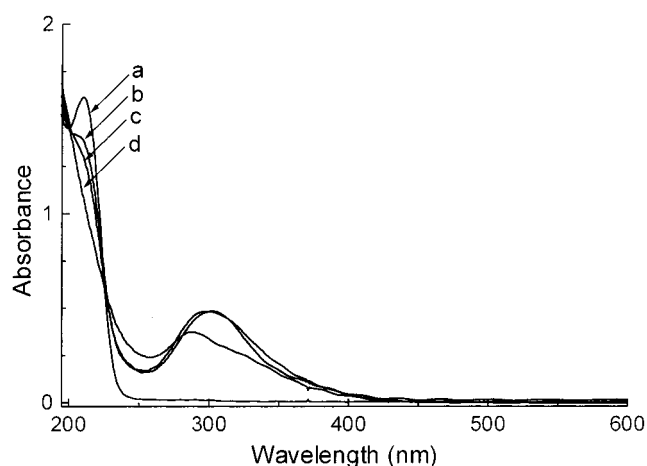


**Figure 2.** UV-visible spectra of GTM films deposited on silica glass with respect to UV curing time: dried (60 °C for 30 min) UV-untreated films (a), UV curing for 5 s (b), 10 s (c), and 20 s (d). Film thickness was  $2.3 \mu\text{m}$ , and both sides of the substrate were coated.

the absorption of C=O attached to saturated hydrocarbons.<sup>32</sup> This result confirms the polymerization of methacrylate groups during UV treatment of the films (Scheme 3).

At the moment we are unable to assign the bands appearing at 225, 235, and 248 nm for the Au-doped

(30) UV-visible spectra of GTM and Au-GTM sols are given as Supporting Information.

(31) Matsuoka, J.; Mizutani, R.; Kaneko, S.; Nasu, H.; Kamiya, K.; Kadono, K.; Sakaguchi, T.; Miya, M. *J. Ceram. Soc. Jpn.* **1993**, *101*, 53.

(32) Dyer, J. R. *Applications of Absorption Spectroscopy of Organic Compounds*; Prentice Hall of India Private Ltd.: New Delhi, 1978.

(33) (a) Herrmann, M.; Kreibig, U.; Schmid, G. *Z. Physik D* **1993**, *26*, S1. (b) Fauth, K.; Kreibig, U.; Schmid, G. *Z. Physik D* **1989**, *12*, 515. (c) Kreibig U.; Vollmer, M. *Optical Properties of Metal Clusters*; Springer, Berlin, 1995; pp 353–354.

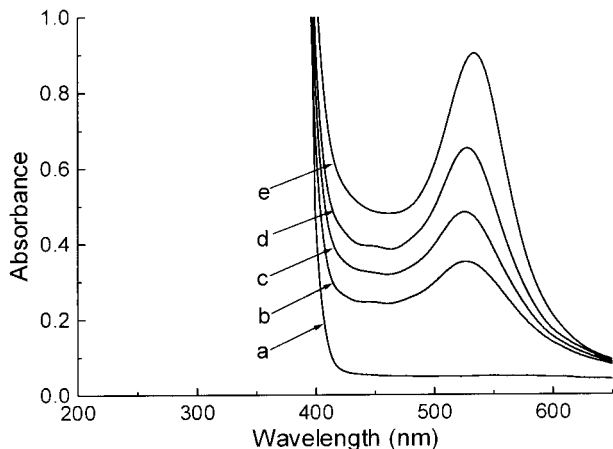
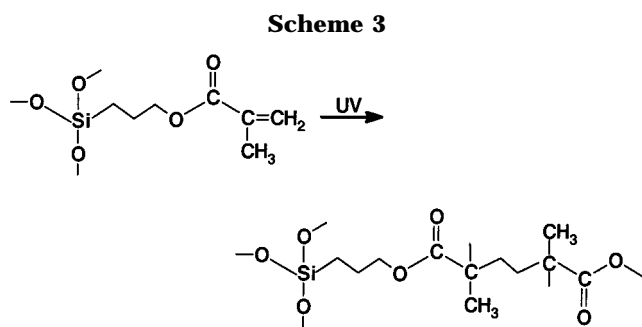


**Figure 3.** Optical absorption spectra of the Au-GTM films deposited on polycarbonate substrates with respect to the UV treatment time: dried (60 °C for 30 min) UV-untreated films (a), UV curing for 5 s (b), 10 s (c), 15 s (d), and 20 s (e). Film thickness was 1.9  $\mu\text{m}$ , and both sides of the substrate were coated.



films. However, these UV bands could be due to the absorption of molecular Au clusters formed with a few of the Au atoms surrounded by organic material.<sup>33</sup> These very small clusters may be formed first as nucleating centers during the exposure to UV radiation, which later agglomerate/coarsen to form relatively large Au nanoclusters. As a consequence, the Au-SPR peak at 530 nm is observed (see Figures 1B and 3).

Optical absorption spectra of the Au-doped inorganic-organic hybrid films deposited on the PC substrate are presented in Figure 3. The film cured in the absence of UV radiation shows no absorption in the visible region, and the corresponding UV-treated films show a clear absorption peak at 530 nm due to the SPR of Au metal nanoclusters, similar to the films deposited on silica substrates (Figure 1B). The gradual increase of peak intensity with UV treatment time (5–20 s) without affecting the SPR peak position suggests a gradual increase in the concentration of the Au nanoclusters. However, no significant increase of the peak intensity was noticed beyond 20 s of irradiation.

**FTIR Spectra.** FTIR spectrum of the Au-GTM sol (Figure 4, curve 1) in the region 2000–1500  $\text{cm}^{-1}$  shows the characteristic peaks for C=O at 1716  $\text{cm}^{-1}$  and C=C<sup>34</sup> at 1638  $\text{cm}^{-1}$  (both from MEMO). The presence of C=C and the position of the carbonyl band (characteristic for  $\alpha,\beta$ -unsaturated ketone<sup>32,35</sup>) indicate that the

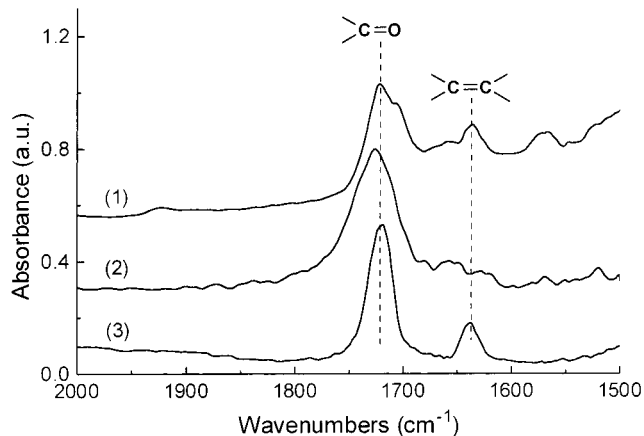


**Figure 4.** FTIR spectra (2000–1500  $\text{cm}^{-1}$ ) of Au-GTM sol (1) and UV cured (20 s) films deposited on a Si wafer (2). The MEMO spectrum (3) is reported for reference.

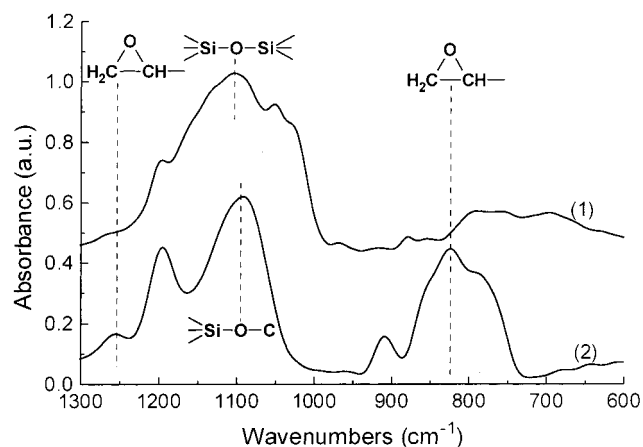


**Figure 5.** FTIR spectrum (1300–600  $\text{cm}^{-1}$ ) of Au-GTM sol (1). The GLYMO spectrum (2) is reported for reference.

methacrylate unsaturation is present in the sol.<sup>36</sup> The UV spectral data also support this (Figure 1).

The FTIR spectrum of the sol in the region 1300–600  $\text{cm}^{-1}$  (Figure 5; curve 1) shows the  $-\text{Si}-\text{O}-\text{Si}-$  asymmetric and symmetric stretching at 1110 and 800  $\text{cm}^{-1}$ ,<sup>37</sup> respectively, and ethanol and methanol peaks (C–O stretch) at 1049 and 1033  $\text{cm}^{-1}$ , respectively. These results support the hydrolysis and condensation of the alkoxy groups, and as a consequence, a silica network is formed in the sol. The sol spectrum (Figure 5) also shows the absence of the epoxide bands<sup>38,39</sup> at 1260–1240  $\text{cm}^{-1}$  (epoxy ring breathing) and 950–810  $\text{cm}^{-1}$  (asymmetrical ring stretching), indicating the polymerization of epoxide groups in the sol. This was expected because epoxy groups polymerize in the presence of 1-methylimidazole and heat.<sup>17,29,40</sup>

Figure 6 shows the evolution of the Si–O–Si asymmetric stretching vibration of the dried (60 and 100 °C) and UV (5 and 20 s) cured films deposited on a Si wafer.

(36) The IR spectrum of MEMO shows C=O at 1718  $\text{cm}^{-1}$  and C=C at 1638  $\text{cm}^{-1}$ .

(37) (a) Duran, A.; Serna, C.; Fornes, V.; Fernandez-Navarro, J. M. *J. Non-Cryst. Solids* **1986**, *82*, 69. (b) De, G.; Kundu, D.; Karmakar, B.; Ganguli, D. *J. Non-Cryst. Solids* **1993**, *155*, 253.

(38) *Comprehensive Heterocyclic Chemistry*; Lwoswski, W., Ed.; Pergamon Press: Oxford, U.K., 1984; Vol. 7, p 99.

(39) *Atlas of Spectral Data and Physical Constants for Organic Compounds*; Grasselli, J. G., Ritchey, W. M., Eds.; CRC Press Inc.: Cleveland, OH, 1975; Vol. I.

(34) Ou, D. L.; Sedden, A. B. *J. Non-Cryst. Solids* **1997**, *210*, 187.

(35) Laren, A.; Matias, M. C.; Orden, M. U.; Urreagu, J. M. *J. Mol. Struct.* **1993**, *294*, 5.

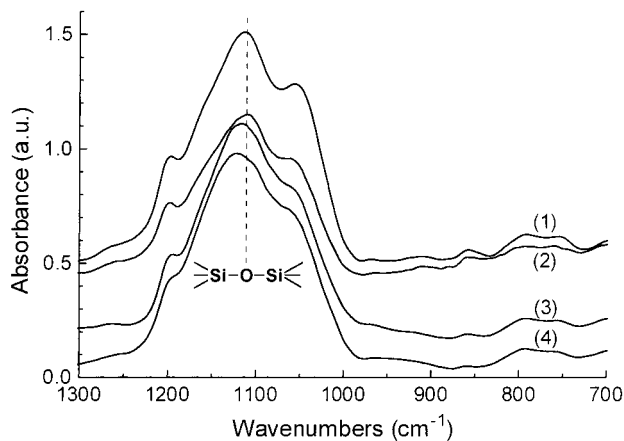


**Figure 6.** FTIR spectra (1300–700  $\text{cm}^{-1}$ ) of Au-GTM films deposited on a Si wafer showing evolution of the  $\text{-Si-O-Si-}$  vibration: (1) deposited film dried at 60 °C for 30 min, (2) 100 °C for 2 h, (3) UV cured for 5 s and (4) 20 s. The spectra of 3 and 4 were taken after the film dried at 60 °C for 30 min.

It has been observed that the 60 °C dried (30 min) film shows a  $\text{Si-O-Si}$  vibration at about  $1110\text{ cm}^{-1}$ , and no shift of this vibration occurred, even after drying at 100 °C. However, this peak gradually shifted to  $1125\text{ cm}^{-1}$  after UV curing for 20 s (no further shifting is observed when the UV-cured films are dried at 100 °C). The shifting of the  $\text{Si-O-Si}$  asymmetric stretching vibration toward a higher wavenumber indicates the strengthening of the silica network through cross-linking<sup>37</sup> during UV curing.<sup>41</sup>

The FTIR spectrum of the UV-cured films also confirmed the polymerization of methacrylate groups. It shows a  $\text{C=O}$  peak at  $1728\text{ cm}^{-1}$  and the absence of the  $\text{C=C}$  peak at  $1638\text{ cm}^{-1}$  (Figure 4, curve 2). The shifting of the  $\text{C=O}$  peak to a longer wavenumber<sup>32</sup> and the absence of  $\text{C=C}$  unsaturation clearly suggest that the polymerization of methacrylate groups (Scheme 3) occurs during UV irradiation.<sup>1e</sup>

**TEM.** A TEM micrograph of the Au-doped film is presented in Figure 7. It clearly shows the presence of spherical (about 8–10 nm diameter) Au nanoclusters in the inorganic–organic film. As shown in the figure, the distribution of the clusters in the film is homogeneous.

**XRD.** An XRD spectrum of Au-GTM films is shown in Figure 8. The peaks at  $2\theta = 38.4^\circ$  and  $44.5^\circ$  are respectively assigned as (111) and (200) reflection lines of fcc Au nanoparticles.<sup>42,43</sup> The mean diameter of the Au nanoparticles calculated from the diffraction bands at  $2\theta = 38.4^\circ$  and  $44.5^\circ$  was found to be about 9 and 9.5 nm, respectively.<sup>42,43</sup> This result also is in agreement with the TEM observations.

**Adhesion and Abrasion of the Au-Nanocluster-Doped Coatings.** The Scotch tape test shows no

(40) Under acidic condition (hydrolysis reaction was initiated in acidic medium and later  $\text{HAuCl}_4$  is used as gold source) the epoxy group may react with water to form diols that cannot be further polymerized to poly(ethylene oxide). In the spectra of sol and film, no diol vibration band at  $4080\text{ cm}^{-1}$  is observed. The absence of epoxide and diol vibrations further indicates the complete polymerization of epoxide groups at the sol stage prior to addition of  $\text{HAuCl}_4$ .

(41) Ohishi, T.; Maekawa, S.; Ishikawa, T.; Kamoto, D. *J. Sol-Gel Sci. Technol.* **1997**, *8*, 511.

(42) Tanahashi, I.; Tohda, T. *J. Am. Ceram. Soc.* **1996**, *79*, 796.

(43) Selvan, S. T.; Nogami, M.; Nakamura, A.; Hamanaka, Y. *J. Non-Cryst. Solids* **1999**, *255*, 254.

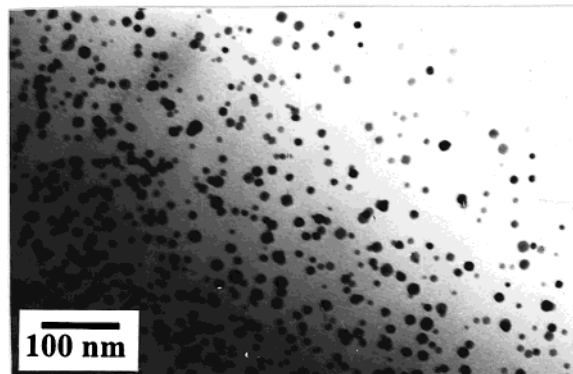


**Figure 7.** TEM image of the UV (20 s), followed by thermally (100 °C) cured Au-GTM films showing presence of spherical Au nanoclusters.

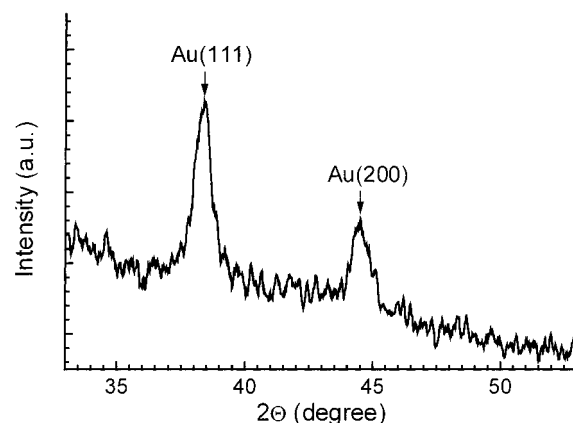


**Figure 8.** XRD spectrum of the UV (20 s), followed by thermally (100 °C) cured Au-GTM films.

peeling off of the coatings when examined under optical microscope using  $100\times$  magnification. This result confirms that the coatings are strongly adhered to the PC substrates. It is known that the  $\text{PC}^{26}$  contains 0.005–0.008% phenolic OH end groups.<sup>44,45</sup> These phenolic OH groups can easily form strong hydrogen bonding with the silanol OH groups present in the sol and gives strong adhesion between the coatings and PC. Other physical adhesion, like van der Waals bonding between the organic part of the coatings and substrates, also contributes for good adhesion.

The abrasion test was done by rubbing the eraser with 2.5 lbs of pressure across the coated and uncoated surfaces. After rubbing, the surface was cleaned with 2-propanol and examined visually and with a profilometer. It was observed that the uncoated substrate (PC) suffered severe damage after only five rubbing (one way) cycles. The surface roughness profiles measured after 5 and 20 rubbing cycles (Figure 9, curves 2 and 3) of uncoated PC show large  $R_a$  values (arithmetical mean of the absolute values of the profile departures within the measured length) of 0.04 and  $0.08\text{ }\mu\text{m}$ , respectively. However, the Au-doped coating ( $5.5\text{ }\mu\text{m}$  thick) showed resistance toward the damage, even after 100 rubbing cycles, whereas only 20 cycles is the specification for

(44) Horbach, A.; Veiel, U.; Wunderlich, H. *Makromol. Chem.* **1965**, *88*, 215.

(45) Freitag, D.; Grigo, U.; Müller, P. R.; Nouvertne, W. In *Encyclopedia of Polymer Science and Engineering*; Kroschwitz, J. I., Ed.; John Wiley and Sons: New York, 1985; Vol. 11, pp 661–662.



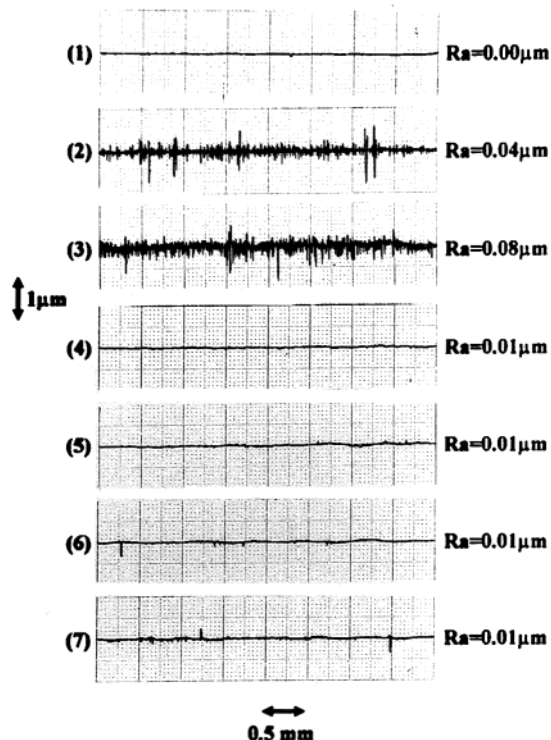


**Figure 9.** Surface profiles of the uncoated polycarbonate and Au-nanocluster-doped hybrid (Au-GTM) film ( $5.5 \mu\text{m}$  thick) coated substrates before and after abrasion with coating hardness tester. Uncoated PC before abrasion (1) and after 5 (2) and 20 cycles of abrasion (3); coated PC before abrasion (4) and after 50 (5), 75 (6), and 100 cycles (7) of abrasion. The corresponding Ra values are shown beside the respective profiles.

optical coatings.<sup>2</sup> The surface roughness profile of coated PC (Figure 9; curve 4) shows an Ra value of  $0.01 \mu\text{m}$  (before abrasion), indicating a smooth surface, and this value remains unchanged after 50–100 abrasion cycles (Figure 9, curves 5–7). The undoped GTM coatings ( $>5 \mu\text{m}$  thick) on PC also showed similar abrasion resistance behavior.

**Structure of Gold Microcrystals Obtained from the Au-GTM Sol.** It should be noted here that the Au-GTM sol remains adequate for coating preparation for about 2 days after preparation, and precipitation of gold microcrystals was observed visually from the sol after about 3–5 days on standing.<sup>27</sup> It is interesting to note that the nucleation and growth of gold crystals is very fast in the sol, and no purple coloration was observed (which is usually observed due to the formation of Au nanoparticles; for details, see ref 24) at any intermediate stages during the precipitation of Au microcrystals. The SEM micrographs (Figure 10a,b) clearly show different shaped gold crystals (triangular, hexagonal, prismatic, etc.). The TEM image of a triangular gold crystal (inset) and its electron diffraction pattern is shown in Figure 10c. The hexagonal diffraction spot pattern clearly suggests that the platelet triangular Au particles were single crystals having a fcc structure with a preferential growth direction along the Au(111) plane.<sup>24</sup> Similar results were obtained when electron diffraction was obtained from a hexagonal crystal. No electron diffraction was observed from the prism-shaped crystals, due to inadequate thickness for penetration of the electron beam.

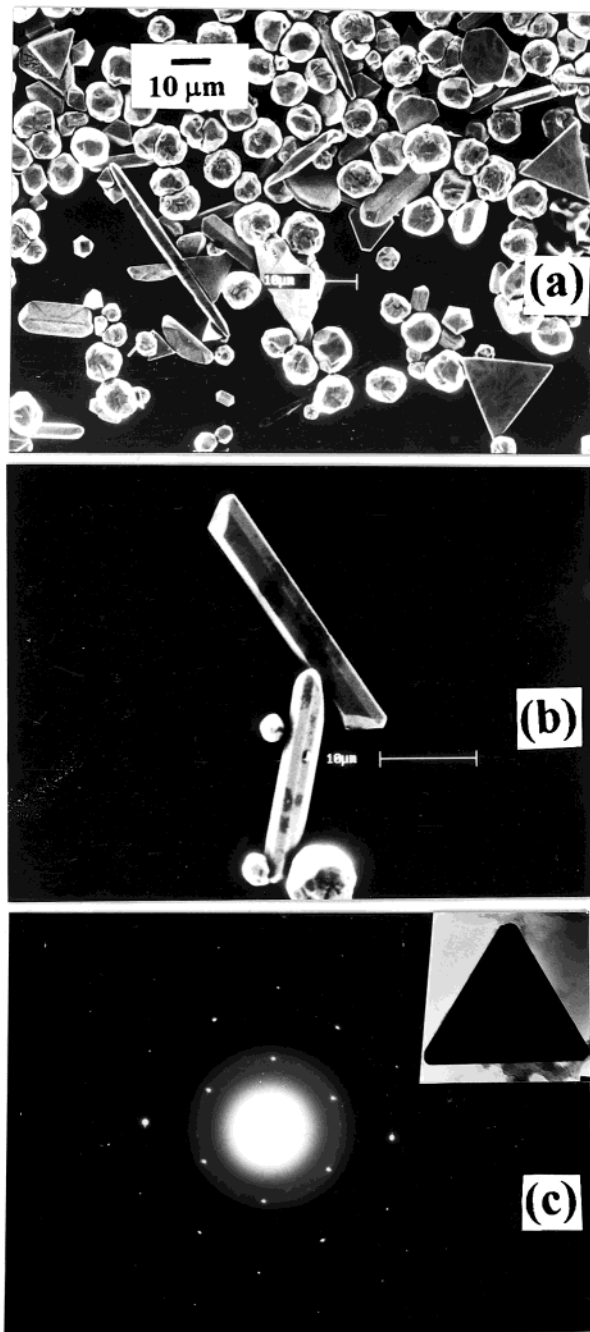


**Figure 10.** SEM images of (a) Au microcrystals showing different shapes, (b) prism-shaped Au microcrystals, and (c) electron diffraction obtained from a triangular Au microcrystals. Inset shows the TEM image of this triangular crystal.

Recently, Zhou et al.<sup>24</sup> reported a shape-controlled synthesis of gold nanoparticles from an aqueous solution of  $\text{HAuCl}_4$  using ultraviolet irradiation. In the present study, shaped gold microcrystals are obtained without the use of UV radiation. To further understand whether this is normal behavior for the crystallization of gold,  $\text{HAuCl}_4$  was incorporated into the TEOS-derived gel (composition 3.4 mol % Au–96.6 mol %  $\text{SiO}_2$ ). The gels during drying at  $50^\circ\text{C}$  cracked catastrophically and irregular-shaped, porous gold microcrystals<sup>46</sup> separated out of the silica matrix. Therefore, it is proposed that

(46) The SEM image of these Au crystals is given as Supporting Information.

the ethanol and methanol present in the sol reduce the gold ions<sup>47</sup> and the hybrid inorganic–organic composite network helps to form the shaped Au crystals in the Au-GTM sol.

### Conclusions

Au nanocluster (8–10 nm) doped inorganic–organic hybrid coatings can be deposited on polycarbonate substrates using a composite GLYMO–TEOS–MEMO sol containing  $\text{HAuCl}_4 \cdot 4\text{H}_2\text{O}$ . The inorganic and organic polymerizable precursors have been linked to each other through an inorganic –Si–O–Si– network following the hydrolysis–condensation of alkoxy groups. The polymerization of the organic part of the precursors leads to sufficient flexibility of the network to apply crack-free thick coatings. UV–visible and FTIR spectroscopy, TEM, and XRD confirmed that the UV curing of the coatings effectively helps simultaneously to reduce the Au ions to metallic nanoclusters, polymerize the methacrylate groups, and strengthen the inorganic silica network. As a result, the Au-doped coatings were

reddish-purple in color and were abrasion-resistant when compared with uncoated PC.

The inorganic–organic hybrid sol acts as a new breeding medium for the generation of shaped Au microcrystals without UV irradiation. The organic solvents present in the sol reduce the Au ions into metallic Au, which grows into shaped microcrystals in the presence of the hybrid network. However, in the films where no organic solvent is available, the formation of gold nanoclusters is induced by UV photoreduction and isolated spherical clusters are formed in a dense cross-linked hybrid matrix.

**Acknowledgment.** We would like to thank Dr. H. S. Maiti, Director, Central Glass & Ceramic Research Institute, for his kind permission to publish this paper. Partial financial support from the Department of Science and Technology, Govt of India, is gratefully acknowledged.

**Supporting Information Available:** UV–visible spectra of GTM and Au-GTM sols, and SEM image of gold crystals obtained from pure silica gel. This material is available free of charge via the Internet at <http://pubs.acs.org>.

CM0100570

---

(47) (a) Ayyappan, S.; Gopalan, R. S.; Subanna, G. N.; Rao, C. N. R. *J. Mater. Res.* **1997**, *12*, 398. (b) Vasani, H. N.; Rao, C. N. R. *J. Mater. Chem.* **1995**, *5*, 1755.